

The lack of conjugation between the vinyl and the porphyrin ring in the ground state is consistent with the heme structure as probed by X-ray crystallography. Little et al.¹³ demonstrated that the 1-methylimidazole Fe(III) porphyrin complex [(1-Melm)₂Fe(PP)]⁺ has a significantly ruffled core with the two vinyl groups rotated out of the pyrrole planes by 24 and 41°. If the vinyls were strongly conjugated they would remain coplanar. Caughy and Ibers¹⁴ also found that the vinyl groups of free base protoporphyrin IX dimethyl ester were not coplanar with the pyrroles. They attributed this lack of planarity as due to steric restraints, between an H_β on the vinyl and the H atoms of adjacent methyl groups, as well as steric interactions between the vinyl H_α and the proximate methine H atom.

It is interesting that the diffuse broad porphyrin $\pi \rightarrow \pi^*$ UV transitions do not give significant resonance enhancement of porphyrin modes. This lack of enhancement probably derives from the large homogeneous line widths that give these transitions such diffuse character.

The large depolarization ratios listed in Table II indicate significant deviations from D_{4h} symmetry for our cyanide complex as well as for similar complexes previously studied by other workers. In fact, the depolarization ratios most consistent with a D_{4h} symmetry were measured for myoglobin.⁴⁷ The large depolarization ratios for the heme ring vibrations obviously indicate breaking of the in-plane x,y degeneracy and a mixing in of nominally B_{1g} or B_{2g} character into the A_{1g} vibrational modes.^{35,45,65,66} On the other hand, the large depolarization ratio of 0.47 measured for the vinyl mode with UV excitation may not be anomalous, since the depolarization ratio of 1,3-hexadiene with 222-nm excitation is 0.45. Although the depolarization ratio should be 0.33

for the vinylic single C=C transition, the larger depolarization ratio is indicative of additional tensor component contributions. Furthermore, the analysis of the depolarization ratio for the two vinyl groups in protoporphyrin IX is complex since it intimately depends upon whether the two vinyl vibrations are coupled. We are presently examining this question.

Conclusions

Our conclusion that there is little conjugation between the vinyl groups and the porphyrin ring in the ground state is suggestive that the vinyl groups have little role in controlling heme reactivity. However, proteins may be able to exercise control on heme reactivity to the extent that the protein perturbation mixes excited-state frontier orbitals of the heme into the ground-state occupied orbitals. For example, the protein could force the vinyl groups to lie planar, and this might mix the vinyl orbitals with the heme orbitals within the ground state. This effect may not be calculable by the techniques of Finsen et al.¹⁵ In fact, recently Gersonde et al.⁴² demonstrated that the vinyl groups in the heme of an insect hemoglobin are so perturbed by the surrounding protein that the two vinyl stretching frequencies split by 7 cm⁻¹.

An obvious conclusion from our study is that one can directly monitor the magnitude of protein-vinyl group interactions by measuring the Soret band enhancement of the vinyl stretching modes. The vinyl mode Soret cross section is directly related to the extent of conjugation. We are in the process of measuring these cross sections in a series of heme proteins.

Acknowledgment. We thank Professor Ken Jordan for many helpful conversations and gratefully acknowledge support of this work from NIH Grant 1R01GM30741-08. Sanford A. Asher is an Established Investigator of the American Heart Association. This work was done during the tenure of an Established Investigatorship of the American Heart Association, Pennsylvania affiliate.

(65) Collins, D. W.; Fitchen, D. B.; Lewis, A. J. *Chem. Phys.* **1973**, *59*, 5714-5719.

(66) Nafie, L. A.; Pezolet, M.; Peticolas, W. L. *Chem. Phys. Lett.* **1973**, *20*, 563-568.

Thermochemical Properties of Gas-Phase MgOH and MgO Determined by Fourier Transform Mass Spectrometry

Lorenza Operti,[†] Edward C. Tews,[‡] Timothy J. MacMahon, and Ben S. Freiser*

Contribution from the Department of Chemistry, Purdue University, West Lafayette, Indiana 47907. Received December 23, 1988

Abstract: Gas-phase thermochemical values $D^{\circ}(\text{Mg}^{+}\text{-OH}) = 75 \pm 4$ kcal/mol, $\text{IP}(\text{MgOH}) = 7.3 \pm 0.1$ eV, $D^{\circ}(\text{Mg}^{+}\text{-O}) = 53 \pm 3$ kcal/mol, and $\text{IP}(\text{MgO}) = 7.9 \pm 0.1$ eV have been experimentally determined by photodissociation measurements and charge-transfer reactions with Fourier transform mass spectrometry. These results, together with previously determined thermochemical data, are used to determine other thermochemical properties of MgOH and MgO. Our value $D^{\circ}(\text{Mg-OH}) = 67 \pm 6$ kcal/mol agrees well with previous experimental values. However, $D^{\circ}(\text{Mg-O}) = 59 \pm 5$ kcal/mol is much lower than previous experimental results, which vary widely, but is in good agreement with a recent ab initio CI calculation.

The thermochemical properties of gas-phase metal monohydroxides have recently been of interest due to the roles these species play in flame chemistry¹ and meteor ablation processes.² Most of the bond dissociation energies of the neutral species have come from flame measurements.³ More recent measurements from Knudsen cell mass spectrometry,⁴⁻⁶ however, have indicated that some of the results reported earlier may be high by as much

as 15 kcal/mol.⁵ Consequently, this study was undertaken to yield another independent measurement of the bond dissociation energy of Mg-OH. Direct measurements were obtained for $D^{\circ}(\text{Mg}^{+}\text{-}$

(1) Hastie, J. W. *High Temperature Vapors-Science and Technology*; Academic: New York, 1975.

(2) (a) Murad, E.; Swider, W. *Geophys. Res. Lett.* **1979**, *6*, 929. (b) Murad, E.; Swider, W.; Benson, S. W. *Nature* **1981**, *289*, 273.

(3) (a) JANAF Thermochemical Tables. *J. Phys. Chem. Ref. Data* **1978**, *7*, 793. (b) Gurvich, L. V.; Ryabova, V. G.; Khitrov, A. N. *Faraday Symp. Chem. Soc.* **1973**, *8*, 83.

(4) Murad, E. *J. Chem. Phys.* **1981**, *75*, 4080.

(5) Murad, E. *Chem. Phys. Lett.* **1980**, *72*, 295.

(6) Murad, E. *J. Chem. Phys.* **1980**, *73*, 1381.

* Author to whom correspondence should be sent.

[†] Present address: Istituto di Chimica Generale ed Inorganica, Università di Torino, Torino, Italy.

[‡] Present address: Abbott Laboratories, Bldg. R1B, Dept. 48T, N. Chicago, IL 60064.

Table I. Supplementary Thermochemical Data^a

species	$\Delta H_f(\text{g})$, kcal/mol	IP, eV
Mg	35.3	
Mg ⁺	211.6	
H	52.10	
H ⁺	365.7	
O	59.6	
OH	9.3 ± 0.3	
H ₂ O	-57.8	
CH ₂ =CHCH ₃	4.8 ± 0.2	
<i>i</i> -C ₃ H ₇	22.3 ± 0.6	7.36 ± 0.02
<i>i</i> -PrOH	-65.1 ± 0.1	
CH ₂ =CHCH ₂ CH ₃	-0.1 ± 0.1	
(<i>Z</i>)-CH ₃ CH=CHCH ₃	-1.9 ± 0.1	
(<i>E</i>)-CH ₃ CH=CHCH ₃	-2.9 ± 0.2	
CH ₂ =C(CH ₃) ₂	-4.0 ± 0.1	
<i>s</i> -C ₄ H ₉	17.0 ± 0.4	7.25 ± 0.02
<i>t</i> -C ₄ H ₉	11.0 ± 0.6	6.70 ± 0.03
<i>s</i> -C ₄ H ₉ ⁺	183	
<i>t</i> -C ₄ H ₉ ⁺	165.8	
<i>s</i> -BuOH	-70.5 ± 0.1	
<i>t</i> -BuOH	-74.7 ± 0.7	

^a Taken from ref 7.

OH) and the ionization potential (IP) of MgOH by photodissociation experiments. These results, along with supplementary thermochemical data,⁷ were used to derive additional thermochemical information for MgOH.

There is also considerable interest in the thermochemical properties of metal monoxides. These species may also play an important role in flames¹ and in stellar atmospheric processes.⁸ Some of the metal monoxide bond energy measurements, which have been obtained by Knudsen cell mass spectrometry, have met with complications due to sample impurities.⁴ Controversies concerning the experimental, as well as the theoretical, bond dissociation energy of Mg-O⁵⁻⁹ have also prompted this work. Direct measurements were obtained for $D^\circ(\text{Mg}^+-\text{O})$ by photodissociation and for IP(MgO) by charge-transfer reactions. These values in turn were used to derive additional thermochemical information on MgO.

Experimental Section

The theory and instrumentation of Fourier transform mass spectrometry (FTMS) have been discussed elsewhere.¹⁰ All experiments were performed with the Nicolet prototype FTMS-1000 previously described in detail¹¹ and equipped with a 5.2-cm cubic trapping cell situated between the poles of a Varian 15-in. electromagnet maintained at 0.9 T. The cell was constructed in our laboratory and utilizes two 80% transmittance stainless steel screens as the transmitter plates. Mg⁺ was generated by focusing the beam of a Quanta Ray Nd:YAG pulsed laser (1064 nm) near the center-drilled hole (~1 mm) of a magnesium rod supported on the transmitter screen nearest to the laser. Details of the laser ionization technique have been described elsewhere.¹²

Chemicals were obtained commercially in high purity and were used as supplied except for multiple freeze-pump-thaw cycles to remove noncondensable gases. All samples were admitted to the cell either through a General Valve Corp. Series 9 pulsed solenoid valve or through a Varian leak valve. Formation of MgO⁺ was accomplished by exciting Mg⁺ to about 15-eV kinetic energy¹³ in the presence of a pulse of N₂O, causing the Mg⁺ to abstract an oxygen atom from N₂O, generating MgO⁺ and N₂ in good yields. Thermalized Mg⁺ is unreactive with N₂O as discussed later. MgOH⁺ was generated by first forming MgO⁺, as

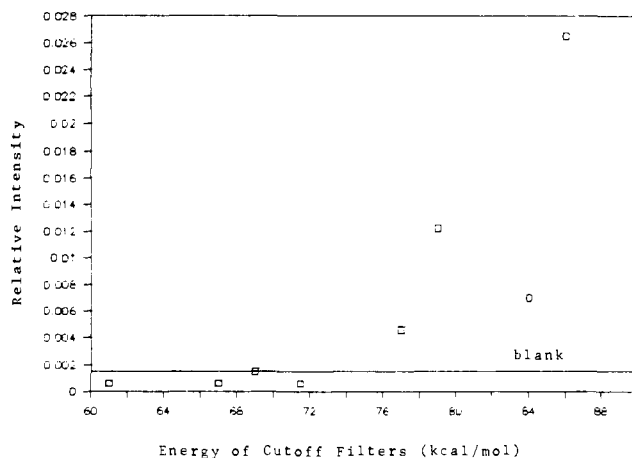


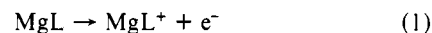
Figure 1. Photodissociation curve for MgOH⁺ with use of sharp cutoff filters.

described above, and then allowing it to react with a pulse of H₂O. Complete conversion of the MgO⁺ to MgOH⁺ was observed. Small amounts of MgOH⁺ could also be produced by exciting Mg⁺ into H₂O. However, much better efficiencies were obtained via MgO⁺.

Photodissociation experiments were performed with a 2.5-kW Hg-Xe arc lamp, used in conjunction with a set of sharp cutoff filters. Bond energy values and error bars were assigned by using the highest energy filter for which photodissociation was not observed and the lowest energy filter for which it was observed and using the centroid for the bond energy and an error bar that included the observed limits. Low pressures were achieved by pulsing in the reagent gases, permitting the ions to be trapped typically for periods of 10–15 s in the absence or presence of light. Prior to isolation, the ions were trapped for ~250 ms in the presence of ~3 × 10⁻⁷ Torr of argon to undergo collisional cooling. However, a small population of excited ions cannot be completely ruled out. Due to the laser shot-to-shot variation, photoappearance of the product ions was monitored and normalized as product ion intensity/parent ion intensity. Further details of the photodissociation experiments can be found elsewhere.¹⁴

Results

The definitions of IP(MgL) and $D^\circ(\text{Mg}^x-\text{L})$ ($x = 0, +1$) are the enthalpies of reactions 1 and 2, respectively, from which eq 3 and 4 are obtained. These equations are used to calculate



$$\Delta H_f(\text{MgL}) = \Delta H_f(\text{MgL}^+) - \text{IP}(\text{MgL}) \quad (3)$$

$$D^\circ(\text{Mg}^x-\text{L}) = \Delta H_f(\text{Mg}^x) + \Delta H_f(\text{L}) - \Delta H_f(\text{MgL}^x) \quad (4)$$

additional thermochemical information from the experimental results, where L = O or OH. Table I contains the supplementary thermochemical information used in these calculations.

Figure 1 shows the photodissociation curve for MgOH⁺, yielding the products Mg⁺ and OH, obtained with the use of cutoff filters. If MgOH⁺ absorbs broadly in the ultraviolet region due to a high density of low-lying electronic states, the photodissociation threshold may yield an absolute bond energy for Mg⁺-OH, as has been the case for a variety of organometallic species.¹⁴ Otherwise, the threshold observed in this experiment yields only an upper limit for this bond energy.¹⁵ The photodissociation threshold is observed to be between 71.5 and 79 kcal/mol, in excellent agreement with a previously reported value of 76 ± 7 kcal/mol (3.3 ± 0.3 eV)⁴ obtained by Knudsen cell mass spectrometry. Therefore, the threshold does appear to be due to thermochemical rather than spectroscopic factors, and $D^\circ(\text{Mg}^+-\text{OH}) = 75 \pm 4$ kcal/mol is assigned, yielding $\Delta H_f(\text{MgOH}^+) = 146 \pm 5$ kcal/mol. For comparison $D^\circ(\text{Fe}^+-\text{OH}) = 73 \pm 3$

(7) Lias, S. G.; Bartmess, J. E.; Liebman, J. F.; Holmes, J. L.; Levin, R. D.; Mallard, W. G. *J. Phys. Chem. Ref. Data Suppl.* **1988**, *17*.

(8) Dirscherl, R.; Michel, K. W.; Cosmovici, C. B. *Astron. Astrophys.* **1978**, *68*, 381.

(9) Bauschlicher, C. W., Jr.; Lengsfeld, B. H., III; Liu, B. *J. Chem. Phys.* **1982**, *77*, 4084.

(10) (a) Comisarow, M. B.; Marshall, A. G. *Chem. Phys. Lett.* **1974**, *26*, 489. (b) Comisarow, M. B. *Adv. Mass Spectrom.* **1980**, *8*, 1698. (c) Freiser, B. S. *Talanta* **1985**, *32*, 697.

(11) Cody, R. B.; Burnier, R. C.; Freiser, B. S. *Anal. Chem.* **1982**, *54*, 96.

(12) Burnier, R. C.; Byrd, G. D.; Freiser, B. S. *J. Am. Chem. Soc.* **1981**, *103*, 4360.

(13) Forbes, R. A.; Lech, L. M.; Freiser, B. S. *Int. J. Mass Spectrom. Ion Processes* **1987**, *77*, 107.

(14) Hettich, R. L.; Jackson, T. C.; Stanko, E. M.; Freiser, B. S. *J. Am. Chem. Soc.* **1986**, *108*, 5086.

(15) Freiser, B. S.; Beauchamp, J. L. *J. Am. Chem. Soc.* **1976**, *98*, 3136.

Table II. Photodissociation Thresholds^a for the Mg(ROH)⁺ Species

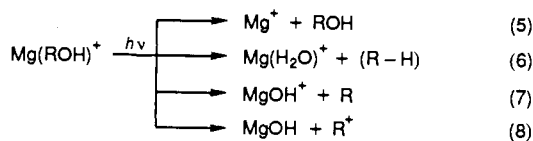
reaction	ROH		
	<i>i</i> -PrOH	<i>s</i> -BuOH	<i>t</i> -BuOH
5	61 < \times < 69	61 < \times < 69	61 < \times < 69
6	61 < \times < 67	61 < \times < 68	67 < \times < 77
7	84 < \times < 86	77 < \times < 84	86 < \times < 92
8		77 < \times < 84	69 < \times < 77

^aThresholds are given in kilocalories per mole.

kcal/mol and $D^\circ(\text{Co}^+-\text{OH}) = 71 \pm 3$ kcal/mol have been previously determined by photodissociation.¹⁶

MgOH⁺ was also trapped in the presence of methanol to see whether a ligand-exchange reaction would occur. No reaction or ligand exchange was observed, which implies $D^\circ(\text{Mg}^+-\text{OH}) > D^\circ(\text{Mg}^+-\text{MeOH}) = 61 \pm 5$ kcal/mol,¹⁷ which is consistent with the photodissociation results although certainly not conclusive by itself.

Further support for this value is obtained by monitoring the processes observed from the photodissociation of Mg(ROH)⁺ (R = *i*-Pr, *s*-Bu, and *t*-Bu), reactions 5–8. Reaction 8 was not



observed from Mg(*i*-PrOH)⁺, while other photodissociation products were formed by loss of H₂ and CH₃^{*} from Mg(*s*-BuOH)⁺ and loss of CH₄ from Mg(*t*-BuOH)⁺. Table II shows the photodissociation thresholds associated with these products, as obtained with sharp cutoff filters, and Table III shows the relative abundances of the same products obtained by white-light photodissociation and by collision-induced dissociation at variable energy. The thresholds observed equal ΔH_{rxn} for each reaction examined. This information, together with some supplemental thermochemical data from Table I, gives $\Delta H_f(\text{Mg(ROH)}^+)$, $\Delta H_f(\text{Mg(H}_2\text{O)}^+)$, $\Delta H_f(\text{MgOH}^+)$, and $\Delta H_f(\text{MgOH})$, which are reported in Table IV. The thresholds for reaction 5 are observed between 61 and 69 kcal/mol, which yield $D^\circ(\text{Mg}^+-\text{ROH}) = 65 \pm 5$ kcal/mol in agreement with $D^\circ(\text{Mg}^+-i\text{-PrOH}) = 65 \pm 5$ kcal/mol previously reported,¹⁷ and $\Delta H_f(\text{Mg(ROH)}^+) = 81 \pm 6$, 76 ± 6 , and 72 ± 6 kcal/mol for R = *i*-Pr, *s*-Bu, and *t*-Bu, respectively. The values of $\Delta H_f(\text{MgOH}^+)$, from reaction 7, give $D^\circ(\text{Mg}^+-\text{OH}) = 77 \pm 7$, 82 ± 7 , and 71 ± 7 kcal/mol for R = *i*-Pr, *s*-Bu, and *t*-Bu, respectively, which are all in good agreement with our photodissociation results directly on MgOH⁺. The ionization potential of MgOH was assigned from the observance of two of the photodissociation processes, reactions 7 and 8, for Mg(*i*-PrOH)⁺ and Mg(*s*-BuOH)⁺. From Table III, observation of reaction 7 exclusively for Mg(*i*-PrOH)⁺ implies $\text{IP}(\text{MgOH}) < \text{IP}(\text{CH}_3\text{CHCH}_3) = 7.36 \pm 0.02$ eV,⁷ while observation of a predominant process (8) from Mg(*s*-BuOH)⁺ indicates $\text{IP}(\text{MgOH}) \geq \text{IP}(\text{CH}_3\text{CH}_2\text{CHCH}_3) = 7.25 \pm 0.02$ eV⁷ from which we assign $\text{IP}(\text{MgOH}) = 7.3 \pm 0.1$ eV. This value is in good agreement with an earlier measurement of $\text{IP}(\text{MgOH}) = 7.5 \pm 0.3$ eV,⁴ in which MgOH was generated by passing hot H₂ over a sample of MgO(s) and its ionization potential measured directly. Further support for this result was provided by a comparison of the enthalpies of reaction 7 and 8 for Mg(*s*-BuOH)⁺ and Mg(*t*-BuOH)⁺. In fact, the difference between the enthalpies of reactions 7 and 8 is the difference between the ionization potentials of MgOH and R, eq 9. The estimated values for $\text{IP}(\text{MgOH})$

$$\Delta H_{\text{rxn}}(7) - \Delta H_{\text{rxn}}(8) = \text{IP}(\text{MgOH}) - \text{IP}(\text{R}) \quad (9)$$

= 7.2 ± 0.2 and 7.4 ± 0.2 eV for R = *s*-BuOH and *t*-BuOH, respectively, are again in excellent agreement with the assigned value. Using $\text{IP}(\text{MgOH}) = 7.3 \pm 0.1$ eV and $\Delta H_f(\text{MgOH}^+) =$

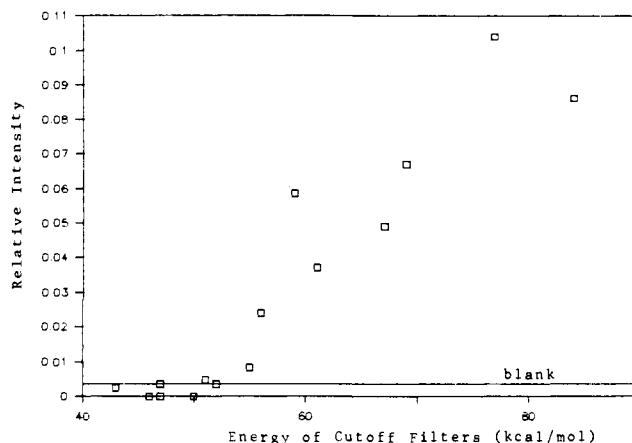
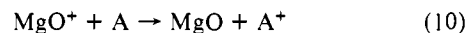


Figure 2. Photodissociation curve for MgO⁺ with use of sharp cutoff filters.

146 ± 5 kcal/mol obtained from the photodissociation results yields $\Delta H_f(\text{MgOH}) = -22 \pm 6$ kcal/mol and $D^\circ(\text{Mg}-\text{OH}) = 67 \pm 6$ kcal/mol. The thresholds for reaction 8 yield $\Delta H_{\text{rxn}} = 80 \pm 4$ and 73 ± 4 kcal/mol for R = *s*-Bu and *t*-Bu, respectively. With these values and $\Delta H_f(\text{Mg(ROH)}^+)$ from above, $\Delta H_f(\text{MgOH}) = -27 \pm 7$ and -21 ± 7 kcal/mol are obtained for R = *s*-Bu and *t*-Bu, respectively, in good agreement with the above results.

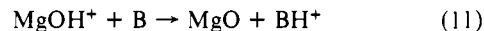
Figure 2 shows the photodissociation curve for MgO⁺, yielding the products Mg⁺ and O, with the use of the cutoff filters. Assuming MgO⁺ absorbs broadly, as MgOH⁺ appears to, the photodissociation threshold, between 50 and 56 kcal/mol, yields $D^\circ(\text{Mg}^+-\text{O}) = 53 \pm 3$ kcal/mol. This result in turn yields $\Delta H_f(\text{MgO}^+) = 218 \pm 3$ kcal/mol. In comparison, a value for $D^\circ(\text{Mg}^+-\text{O}) = 33 \pm 8$ kcal/mol¹⁸ has been reported, with an ICR spectrometer, which was obtained by monitoring oxygen atom transfer to thermalized Mg⁺ from O₃ and N₂O. Here, the upper limit of 40 kcal/mol was assigned since no reaction was observed with N₂O. However, kinetic rather than thermodynamic factors are probably responsible for the lack of reaction.¹⁹

IP(MgO) was determined by monitoring charge-transfer reaction 10. Table V lists the series of compounds used in this study.



Charge transfer was not observed for compounds that had $\text{IP} \geq 7.95$ eV, while compounds with $\text{IP} \leq 7.82$ eV all proceeded as shown in reaction 10 to yield the charge transfer product. Therefore, $\text{IP}(\text{MgO}) = 7.9 \pm 0.1$ eV has been assigned, yielding $\Delta H_f(\text{MgO}) = 36 \pm 5$ and $D^\circ(\text{Mg}-\text{O}) = 59 \pm 5$ kcal/mol.

A limit for the proton affinity (PA) of MgO was determined by monitoring reaction 11 with a variety of bases. Since no



reaction was observed for MgOH⁺ with *N,N,N',N'*-tetramethyl-1,8-naphthalenediamine, often referred to as the Proton Sponge, $\text{PA}(\text{MgO}) > 241.8$ kcal/mol²¹ has been assigned. This result is consistent with an estimated value of $\text{PA}(\text{MgO}) = 256 \pm 7$ kcal/mol obtained with the use of the assigned values of $\Delta H_f(\text{MgOH}^+)$ and $\Delta H_f(\text{MgO})$.

Finally, $D^\circ(\text{MgO}^+-\text{H}) = 124 \pm 7$ kcal/mol can be calculated with eq 12 and the results from this study, which is in accord with the occurrence of reaction 13. This process was used to form

$$D^\circ(\text{MgO}^+-\text{H}) = \Delta H_f(\text{MgO}^+) + \Delta H_f(\text{H}) - \Delta H_f(\text{MgOH}^+) \quad (12)$$



(18) Kappes, M. M.; Staley, R. H. *J. Phys. Chem.* **1981**, *85*, 942.

(19) Armentrout, P. B.; Halle, L. F.; Beauchamp, J. L. *J. Chem. Phys.* **1982**, *76*, 2449.

(20) Rosenstock, H. M.; Draxl, K.; Steiner, B. W.; Herron, J. T. *J. Phys. Chem. Ref. Data Suppl.* **1977**, *6*.

(21) Lias, S. G.; Liebman, J. F.; Levin, R. D. *J. Phys. Chem. Ref. Data* **1984**, *13*, 804.

(16) Cassady, C. J.; Freiser, B. S. *J. Am. Chem. Soc.* **1984**, *106*, 6176.

(17) Operti, L.; Tews, E. C.; Freiser, B. S. *J. Am. Chem. Soc.* **1988**, *110*, 3847.

Table III. Relative Abundances of the Products of White Light Photodissociation (PDS) and of Collision-Induced Dissociation (CID) from the Mg(ROH)⁺ Species

reaction	<i>i</i> -PrOH			<i>s</i> -BuOH			<i>t</i> -BuOH		
	PDS	CID		PDS ^a	CID		PDS ^b	CID	
		16 eV	40 eV		14 eV	43 eV		14 eV	43 eV
5	17	31	58	10	52	56	7	14	40
6	81	69	42	57	48	44	51	86	38
7	2			7			3		9
8				26			39		13

^a Loss of H₂ and CH₃ also observed. ^b Loss of CH₄ also observed.

Table IV. Thermochemical Data Calculated from Photodissociation Thresholds of Mg(ROH)⁺ Species

reaction	ΔH_f^a	ROH		
		<i>i</i> -PrOH	<i>s</i> -BuOH	<i>t</i> -BuOH
5	Mg(ROH) ⁺	81 ± 6	76 ± 6	72 ± 6
6	Mg(H ₂ O) ⁺ ^b	140 ± 7	142 ± 7	148 ± 7
7	MgOH ⁺	144 ± 7	139 ± 7	150 ± 7
8	MgOH		-27 ± 7	-21 ± 7

^a ΔH_f are given in kilocalories per mole. ^b For more details on ΔH_f (Mg(H₂O)⁺), see text.

Table V. Charge-Transfer Data for MgO⁺

compound	ionization potential, ^a eV	observation of charge transfer
W(CO) ₆	8.24 ^b	no
(C ₂ H ₅) ₂ NH	8.01	no
Fe(CO) ₅	7.95 ^b	no
(CH ₃) ₃ N	7.82	yes
(C ₂ H ₅) ₃ N	7.50	yes
ferrocene	6.97 ^b	yes

^a Ionization potentials taken from ref 7 unless otherwise noted.

^b Taken from ref 20.

MgOH⁺ in the ion source and gave complete conversion of MgO⁺ to MgOH⁺, implying $D^\circ(\text{MgO}^+-\text{H}) > D^\circ(\text{HO}-\text{H}) = 119$ kcal/mol.⁷ This bond energy is closer to $D^\circ(\text{O}-\text{H}) \sim 102$ kcal/mol²⁰ than $D^\circ(\text{Mg}^+-\text{H}) \sim 46$ kcal/mol,²² which implies a Mg⁺-OH structure, as expected. Table VI summarizes the results obtained in this study and compares them to previously published results.

The photodissociation threshold for reaction 6 should yield $\Delta H_f(\text{Mg}(\text{H}_2\text{O})^+)$, which has been calculated to be 140 ± 7, 142 ± 7, and 148 ± 7 kcal/mol for R = *i*-Pr, *s*-Bu, and *t*-Bu, respectively. From these results, $D^\circ(\text{Mg}^+-\text{H}_2\text{O})$ seems to be in the range 0–24 kcal/mol. However, direct photodissociation of Mg(H₂O)⁺ to Mg⁺ yields a threshold of $D^\circ(\text{Mg}^+-\text{H}_2\text{O}) = 60 \pm 5$ kcal/mol, which is supported by an estimate of $D^\circ(\text{Mg}^+-\text{H}_2\text{O}) = 56 \pm 5$ kcal/mol obtained on the basis of the correlation of Mg⁺ affinity with proton affinity.¹⁷ A possible explanation for this discrepancy is the formation of a reaction intermediate or activated complex, and thus the existence of an energy barrier when Mg(H₂O)⁺ is formed from Mg(ROH)⁺. At some time during the dissociation process, transfer of an H atom to the oxygen takes place. This could conceivably involve an intermediate having a different structure (such as a hydride hydroxide structure) and a higher formation enthalpy, $\Delta H_f \cong 144$ kcal/mol, than the isomeric Mg(H₂O)⁺ ion, $\Delta H_f \cong 96$ kcal/mol, formed by the reaction of Mg⁺ with water. No additional experimental evidence could be obtained to support this hypothesis. However, regardless of any intermediate structures, the final product of reaction 6 is the more stable Mg(H₂O)⁺ ion.

Discussion

Perusal of Table VI illustrates that there is a variety of experimentally determined values for $D^\circ(\text{Mg}-\text{OH})$. These values range from 56 ± 5²³ to ≤90 kcal/mol²⁴ from flame measurements,

(22) $D^\circ(\text{Mg}^+-\text{H})$ is estimated to be approximately $D^\circ(\text{Ca}^+-\text{H}) = 45.9 \pm 2$ kcal/mol. Schilling, J. B.; Goddard, W. A., III; Beauchamp, J. L. *J. Am. Chem. Soc.* **1986**, *108*, 582.

Table VI. Summary of Thermochemical Data Obtained in This Study in Comparison to Previously Reported Values^a

	this study	previously reported	ref
$D^\circ(\text{Mg}^+-\text{OH})$	75 ± 4	76 ± 7	4
$\Delta H_f(\text{MgOH}^+)$	146 ± 5		
IP(MgOH)	(7.3 ± 0.1) ^c	(7.5 ± 0.3) ^c	4
$\Delta H_f(\text{MgOH})$	168 ± 3	173 ± 7	4
$D^\circ(\text{Mg}-\text{OH})$	-22 ± 8	-29 ± 5	23
	67 ± 6	56 ± 5	4
		74 ± 5	4
		83 ± 52	5
		≤90	24
$D^\circ(\text{Mg}^+-\text{O})$	53 ± 3	[46 ± 12] ^b	4
		33 ± 8	21
$\Delta H_f(\text{MgO}^+)$	218 ± 3	[224 ± 12]	4
		238 ± 8	21
IP(MgO)	(7.9 ± 0.1) ^c	[9.2 ± 0.5] ^c	4
	182 ± 2	212 ± 12	
$\Delta H_f(\text{MgO})$	36 ± 5	[12 ± 17]	4
$D^\circ(\text{Mg}-\text{O})$	59 ± 5	98 ± 2	23
		96 ± 2	24
		86 ± 5	26
		80 ± 6	3a
		61 ± 4	9
$D^\circ(\text{MgO}^+-\text{H})$	124 ± 7	[134 ± 18]	4

^a In kilocalories per mole unless noted. ^b The values in brackets are estimated in ref 4. ^c In electronvolts.

with a value of 74 ± 5 kcal/mol⁴ reported from Knudsen cell mass spectrometry. A value of 83 ± 5 kcal/mol²⁵ was also obtained from theoretical calculations based on pseudo-halide models. Since photodissociation experiments yield upper limits for bond energies, our value of $D^\circ(\text{Mg}^+-\text{OH}) = 75 \pm 4$ kcal/mol, which implies $D^\circ(\text{Mg}-\text{OH}) = 67 \pm 6$ kcal/mol, provides an upper limit. This result suggests that the 83 ± 5 kcal/mol²⁵ value based on pseudo-halide theory is too high, while the result ≤90 kcal/mol²⁴ from flame measurements is at least consistent. Finally, the value 74 ± 5 kcal/mol,⁴ obtained from Knudsen cell mass spectrometry, is in good agreement with our results. As a consequence, the ionization potential of MgOH also agrees well with the determination from Knudsen cell mass spectrometry. These results tend to imply that thermodynamic thresholds are obtained by photodissociation of MgOH⁺ and that $D^\circ(\text{Mg}-\text{OH}) \sim 70$ kcal/mol.

Perusal of the MgO data in Table VI indicates that there are also discrepancies in $D^\circ(\text{Mg}-\text{O})$. Flame measurements seem to agree with each other at ~98 kcal/mol,^{23,24} while a value of 86 kcal/mol²⁶ has been determined by Knudsen cell mass spectrometry. Problems occur due to impurities in the MgO samples in the Knudsen cell experiment, so that these values may be a bit misleading. A theoretical value of 61 ± 4 kcal/mol⁹ has been determined by ab initio CI calculations. Our value of $D^\circ(\text{Mg}^+-\text{O}) = 53 \pm 3$ kcal/mol implies $D^\circ(\text{Mg}-\text{O}) = 59 \pm 5$ kcal/mol. Thus, $D^\circ(\text{Mg}-\text{O})$ determined from flame and Knudsen cell measurements may be high, while the theoretical value of 61 ± 4 kcal/mol⁹ is in excellent agreement with our results.

(23) Bulewicz, E. M.; Sugen, T. M. *Trans. Faraday Soc.* **1959**, *55*, 720.
 (24) Cotton, D. H.; Jenkins, D. R. *Trans. Faraday Soc.* **1969**, *65*, 376.
 (25) Chase, M. W., Jr.; Curnutt, J. L.; McDonald, R. A.; Syverud, A. N. *J. Phys. Chem. Ref. Data* **1978**, *7*, 793.
 (26) Drowart, J.; Exsteen, G.; Veerhagen, G. *Trans. Faraday Soc.* **1964**, *60*, 1920.

Conclusions

Values of $D^{\circ}(\text{Mg}^{+}\text{-OH}) = 75 \pm 4$ kcal/mol and $D^{\circ}(\text{Mg}^{+}\text{-O}) = 53 \pm 3$ kcal/mol were obtained from photodissociation thresholds. $D^{\circ}(\text{Mg}^{+}\text{-OH})$ is in excellent agreement with Murad's experimental results^{4,5} indicating that the photodissociation thresholds for MgL^{+} species can yield absolute bond energy information. The $\text{IP}(\text{MgOH}) = 7.3 \pm 0.1$ eV was also determined by photodissociation experiments, while $\text{IP}(\text{MgO}) = 7.9 \pm 0.1$ eV was determined by charge-transfer reactions. With the use of these experimental results, a variety of other thermochemical values for MgOH and MgO were obtained and summarized in Table VI. Also, our results are in excellent agreement with the ab initio calculations⁹ on MgO and may imply that the experi-

mental results obtained from both flame measurements^{23,24} and Knudsen cell mass spectrometry²⁶ are high, possibly due to sample impurities.

In view of these results, the use of photodissociation experiments continues to play an important role for the determination of organometallic bond energies.

Acknowledgment is made to the Division of Chemical Sciences in the Office of Basic Energy Sciences in the U.S. Department of Energy (Grant DE-FG02-87ER13766) and to the National Science Foundation (Grant CHE-8612234) for supporting this research. L.O. thanks the Consiglio Nazionale delle Ricerche (Italy) and E.C.T. thanks Lawrence Livermore National Laboratory for providing fellowship support.

Surface-Enhanced Resonance Raman Scattering Spectroscopy Applied to Phytochrome and Its Model Compounds. 1. Biliverdin Photoisomers

Randall E. Holt, David L. Farrens, Pill-Soon Song,* and Therese M. Cotton*

Contribution from the Department of Chemistry and Institute for Cellular and Molecular Photobiology, University of Nebraska—Lincoln, Lincoln, Nebraska 68588-0304.

Received January 13, 1989

Abstract: The application of surface-enhanced resonance Raman scattering (SERRS) spectroscopy to the analysis of the configuration of biliverdin dimethyl ester (BVDE) is reported. SERRS spectra obtained by adsorption of the compounds onto an electrochemically roughened silver electrode and recorded at 77 K were intense and free of significant photodegradation. The similarity of the SERRS and resonance Raman (RR) spectra obtained under identical conditions suggests that no perturbation of the electronic structure of the BVDE occurs upon interaction with the silver surface, and that the distribution of conformers comprising the BVDE solution is not changed. SERRS spectra of the deuterated and monoprotonated Z,Z,Z isomer are also presented. To investigate the influence of configuration upon the Raman spectrum we have synthesized and purified the E,Z,Z and Z,Z,E isomers of BVDE. Excellent SERRS spectra were obtained from the solutions of the compounds eluted directly from the TLC plates. Comparison of these isomers to the more stable Z,Z,Z isomer reveals differences in frequencies and relative intensities associated with the change in molecular geometry upon isomerization. Most significant is the change in intensity of bands observed at 1255 and at 1245 cm^{-1} , a band that has been previously correlated to changes in conformation of the closely related phycocyanin chromophore.

Biliverdin, a bile pigment, has attracted attention recently as a model compound for the chromophores associated with the light-harvesting antenna pigments known as the phycocyanins, which are found in red algae, cyanobacteria, and cryptophytes, and the photoreceptor pigments associated with photomorphogenesis (phytochrome in higher plants) and chromatic adaptation ("adaptachromes" in cyanobacteria and red algae).¹ The structures of the phycocyanin chromophores are relatively well characterized for only a few phycobiliproteins. The structure of the red-absorbing form of phytochrome, Pr, has been established with confidence² and that of the far-red-absorbing form, Pfr, with less confidence.³ In both of these types of biliproteins, the configurations about the C=C double bonds and the conformation of the molecule produced by rotation about the single C—C bonds appear to be extremely important in producing the spectroscopic properties required by the organism for the biliproteins' specialized function. Consequently, biliverdin has become the focus for a number of spectroscopic investigations⁴ and theoretical calcula-

tions⁵ aimed at providing insight into the dependence of the spectroscopic properties of these biliverdin-type chromophores upon their molecular geometry.

Resonance Raman (RR) spectroscopy has enjoyed success as a method of analysis of chromophore-containing molecules of biological interest.⁶ The combination of excellent sensitivity and selectivity for only the chromophoric group allows vibrational spectra to be observed in solutions of relatively low concentrations

(1) (a) Glazer, A. N. *Biochim. Biophys. Acta* **1984**, *768*, 29-51. (b) Scheer, H. *Angew. Chem., Int. Ed. Engl.* **1981**, *20*, 241-261.

(2) Lagarias, J. C.; Rapoport, H. *J. Am. Chem. Soc.* **1980**, *102*, 4821-4828.

(3) Rüdiger, W.; Thümmel, F.; Cmiel, E.; Schneider, S. *Proc. Natl. Acad. Sci. U.S.A.* **1983**, *80*, 6244-6248.

(4) (a) Chae, Q.; Song, P.-S. *J. Am. Chem. Soc.* **1975**, *97*, 4176-4179. (b) Braslavsky, S. E.; Holzwarth, A. R.; Schaffner, K. *Angew. Chem., Int. Ed. Engl.* **1983**, *22*, 656-674. (c) Al-Ekabi, H.; Tegmo-Larsson, I.-M.; Braslavsky, S. E.; Holzwarth, A. R.; Schaffner, K. *Photochem. Photobiol.* **1986**, *44*, 433-440. (d) Braslavsky, S. E.; Al-Ekabi, H.; Petrier, C.; Schaffner, K. *Photochem. Photobiol.* **1985**, *41*, 237-246. (e) Holzwarth, A. R.; Wendler, J.; Schaffner, K.; Sundström, V.; Sandström, A.; Gillbro, T. *Isr. J. Chem.* **1983**, *23*, 223-231. (f) Braslavsky, S. E.; Holzwarth, A. R.; Langer, E.; Lehner, H.; Matthews, J. I.; Schaffner, K. *Isr. J. Chem.* **1980**, *20*, 196-202. (g) Braslavsky, S. E.; Ellul, R. M.; Weiss, R. G.; Al-Ekabi, H.; Schaffner, K. *Tetrahedron* **1983**, *39*, 1909-1913.

(5) (a) Scheer, H.; Formanek, H.; Schneider, S. *Photochem. Photobiol.* **1982**, *36*, 259-272. (b) Falk, H.; Höllbacher, G. *Monatsh. Chem.* **1978**, *109*, 1429-1449. (c) Falk, H.; Müller, N. *Tetrahedron* **1983**, *39*, 1875-1885.

(6) (a) Spiro, T. G., Ed.; *Biological Applications of Raman Spectroscopy*; John Wiley and Sons: New York, 1987. (b) Carey, P. R. *Biochemical Applications of Raman and Resonance Raman Spectroscopies*; Academic Press: New York, 1982.